Journal of Alloys and Compounds 509 (2011) 1206–1210

Contents lists available at ScienceDirect

Journal of Alloys and Compounds

journal homepage: www.elsevier.com/locate/jallcom

XRD simulation study of doped $LiFePO_4$

Dongyun Zhang[a,b], Peixin Zhang[a,c,*], Juan Yi[c], Qiuhua Yuan[c], Jianhui Jiang[d], Qiming Xu[a], Zhongkuan Luo[c], Xiangzhong Ren[c]

[a] School of Materials Science and Engineering, Xi'an University of Architecture and Technology, Xi'an 710055, PR China
[b] School of Chemistry and Chemical Engineering, Guangxi University, Nanning 530004, PR China
[c] School of Chemistry and Chemical Engineering, Shenzhen University, Shenzhen 518060, PR China
[d] College of Chemistry and Chemical Engineering, Hunan University, Changsha 410082, PR China

ARTICLE INFO

Article history:
Received 20 May 2010
Received in revised form
25 September 2010
Accepted 28 September 2010
Available online 8 October 2010

Keywords:
Lithium-ion batteries
$LiFePO_4$
XRD
Simulation
Doping

ABSTRACT

$LiFePO_4$ has become a highly promising cathode material for use in the next generation of lithium-ion batteries, in which metal-doping is typically employed to improve the electrochemical properties. However, it is always difficult to resolve the issue that how the doping element and its position cause the microstructural changes and eventually influence the material properties. In this work, the X-ray diffraction (XRD) patterns of a series of metal-doped $LiFePO_4$ were simulated by software MS Reflex to investigate those factors since XRD is a typical technique for the study of crystal structures. The effect of simulation conditions, doping position, and types of doping elements were discussed. The results revealed that: (1) the suitable step size should be 0.02° or less, and the simulation position had little influence on the XRD pattern; (2) the peak intensity changed with doping position, and had been affected more evidently at the Li-site compare with the Fe-site; (3) there was a close relationship between the doping elements and peak intensities in XRD patterns, and the variation degree of the peak intensity increased linearly with the atomic number of doping elements.

1. Introduction

The olivine-type $LiFePO_4$ has attracted much attention as the cathode of rechargeable lithium-ion battery with some remarkable advantages such as inexpensiveness, environmental friendliness, appropriate working voltage (3.4 V), and handling or operational safety. However, $LiFePO_4$ shows poor electronic conductivity and small lithium ion diffusivity, resulting from the structural arrangement characteristics, which is an obstacle when applied in high power batteries [1,2]. To overcome these problems, a variety of solutions have been proposed including carbon-coating on $LiFePO_4$ surface [3–5], metal-doping [6,7] and synthesizing products with fine particles [8,9]. Among them, a lot of experiments concerning metal-doped $LiFePO_4$, such as V [7,10,11], Mn [12–14], Zn [15] and Ru [16], have been carried out since it was first introduced by Chung [17]. The material structures and relevant electrochemical performances could be influenced significantly even though the doping amount is relatively small. Moreover, studies indicated that the diffusion of Li ions was influenced by doping elements and their position within the lattice [18–21]. So it is important to determine the structure variety, especially whether the dopants occupy Li-site or Fe-site.

Recently, various instrumental analysis techniques such as XRD refinement [6,10], extended X-ray absorption fine-structure (EXAFS) [22,23], X-ray absorption near-edge spectroscopy (XANES) [22–25], and neutron diffraction [26–28], are adopted to analyze and identify the types or sites of doping atoms in $LiFePO_4$. Among these, the neutron diffraction is considered to be the most accurate method, but it is not widely used because of comparatively high cost. In contrast, XRD is the most common technique for crystal structural analysis. As a result, the variance of XRD spectra is found to be closely related to the positioning or amount of doped elements. The computer simulation of the XRD spectra may be an effective and low-cost approach to be employed to analyze the location or quantity of doping metal, by which a better understanding of the crystal microstructural change after doping could be obtained [18,29].

There are many elements available for dopants [6,7,10–17,30], so it may cost a lot of energy if all of them are to be tested. At present, the analysis of XRD is only used for roughly qualitative analysis, and there is no report about the relationship between doped elements and variation of XRD spectra. In this paper, the XRD simulation was carried out through the suitable software, focusing on the variations of XRD spectra resulting from different doping elements or sites (Li-site and Fe-site) in $LiFePO_4$. And the changes of intensities

* Corresponding author at: School of Chemistry and Chemical Engineering, Shenzhen University, Shenzhen 518060, China. Fax: +86 755 26558134.
E-mail address: pxzhang96@yahoo.com (P. Zhang).

0925-8388/$ – see front matter © 2010 Elsevier B.V. All rights reserved.
doi:10.1016/j.jallcom.2010.09.186

of main diffraction peaks were investigated, which may provide theoretical foundation for the study of the relationship between the microstructures and relevant properties of doped $LiFePO_4$.

2. Simulation method

The calculation was carried out by using the Powder Diffraction function in Reflex module included in software Materials Studio. Reflex is a module that can be used to simulate and analyze the data of X-ray, electron, and neutron diffraction. And it may provide the suitable tools to extract the maximum amount of information from diffraction patterns of most compounds such as organic, inorganic, organ metallic, and biological crystals.

The crystal structural parameter of $LiFePO_4$, referred to the JCPDS standard database (PDF83-2092 [31]), has proved to be reasonable through the first principles calculation. The space structural model of M (i.e. doping metal) occupying the Li- and Fe-substitute site is established by placing M atom into the corresponding positions in the internal lattice of standard $LiFePO_4$. Different doping amount could be achieved by replacing different amount of Li or Fe in a variety of supercells.

There are three types of doping position including Li-site ($Li_{1-x}M_xFePO_4$), Fe-site ($LiFe_{1-y}M_yPO_4$), and both sites ($Li_{1-x}M_{x+y}Fe_{1-y}PO_4$), which were discussed in this paper. For example, if one Li atom is replaced by one Nb atom in supercell (3 3 3), the simulation model is $Li_{1-1/108}Nb_{1/108}FePO_4$ because there are 108 Li atoms in supercell (3 3 3). The molar content of Nb in this system should be 0.926% (=1/108). Similarly $Li_{1-5/256}Nb_{5/256+32/256}Fe_{1-32/256}PO_4$ indicates that 5 Li and 32 Fe are replaced by Nb in supercell (4 4 4), and the doping molar contents of Li and Fe are 1.95% and 12.5% respectively.

3. Results and discussion

3.1. Conditions of simulation

3.1.1. Different modeling step size

As we know, the XRD results are mainly determined by the following parameters: scanning velocity, time constants (step size) and feeding speed. The diffraction analysis is based on the data collected by the statistical average, which is significantly dependent on the variance of time and space. Generally, the longer the scanning time, the more accurate the results, however, this tends to cause a longer testing time. On the other hand, the collected peaks may be more difficult to distinguish due to a big step size, and thereby it is no good for characterization. So it is necessary to choose a suitable step size for XRD simulation first.

Fig. 1 illustrates the simulation results for single crystal under different step sizes (0.05, 0.02, 0.01, and 0.001). When 0.05° was chose as the step size, it is evidently shown that there existed a big difference in the peak intensities compared to the standard data. For example, the biggest peak intensity is observed at 25.55°, which should be at 35.585° according to PDF83-2092. Whereas it is both observed at 35.58° when step size are 0.01° and 0.02°, and the result for step size 0.001° is 35.585°, which is the closest to standard data. This indicates that when the step size is 0.001°, 0.01°or 0.02°, the simulation results show good agreement with the standard spectrum, including the peak positions and the order of the five highest peaks. Thus the step size should be chosen among 0.02°, 0.01° or 0.001°. Since 0.01° and 0.001° may prolong the testing time and cause too many data to process, 0.02° should be reasonably selected as the suitable step size for this study.

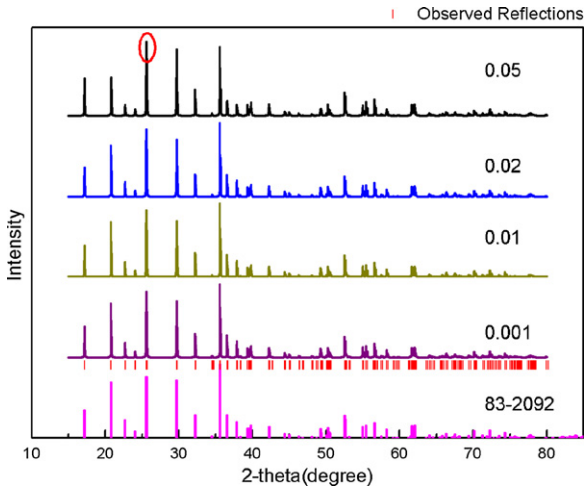

Fig. 1. Simulated XRD pattern of $LiFePO_4$ at different step size.

3.1.2. Different simulation positions

Since the position of doping metal could be at Li-site, Fe-site or both sites in $LiFePO_4$, the specific location of doping can only be approximately determined by XRD refinement. And it is rather difficult to determine the doping position or quantity precisely due to the limitation of technology development and other aspects. Instead, it can be solved successfully by means of the computer simulation.

According to the characteristic of $LiFePO_4$ crystal structure, there are 32 Li atoms in super cell (2 2 2) which can be divided into 8 groups of positions (Fig. 2(a)). Fig. 2(b) shows the simulated XRD spectra of $Li_{1-4/32}Nb_{4/32}FePO_4$, there is hardly any difference

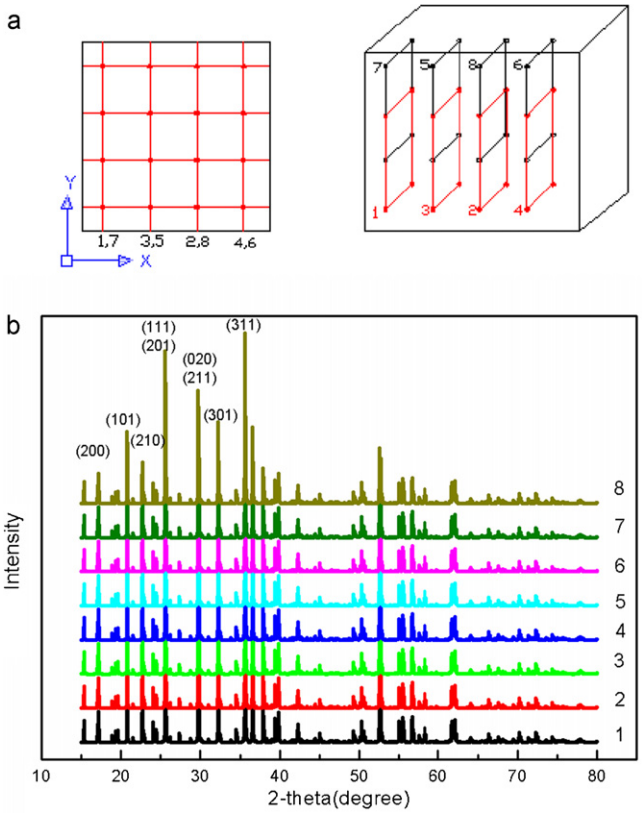

Fig. 2. (a) Distribution position of Li in supercells (2 2 2). (b) Simulated XRD pattern of $LiFePO_4$ at different simulation positions.

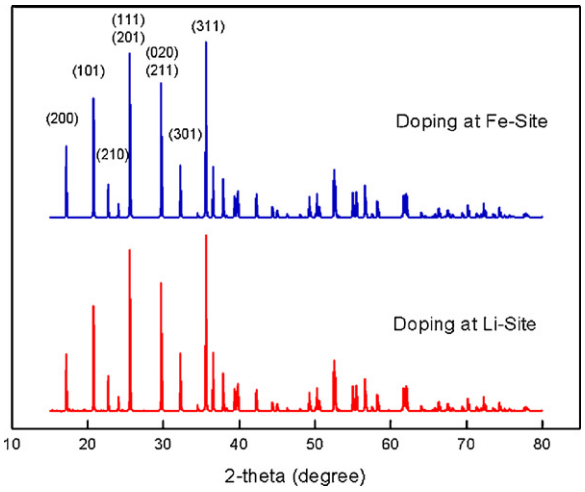

Fig. 3. Simulated XRD pattern of Nb-doped $LiFePO_4$.

among the main peaks (position and intensity) when Nb doped at different positions. So it may be noted that the simulation positions of doping atom have little influence on the simulated XRD spectra.

3.2. The effect of dopants on XRD spectra

3.2.1. Different doping positions

In this paper, the XRD spectra of $LiFePO_4$ with different doping positions were studied through models $Li_{1-4/256}Nb_{4/256}FePO_4$ and $LiFe_{1-4/256}Nb_{4/256}PO_4$ (i.e. 4 Nb replacing the Li-site and Fe-site in the supercell (4 4 4)), see Fig. 3.

Fig. 4 shows the changes of peak intensities, where Δ represents the value of doped simulated intensity minus that of undoped $LiFePO_4$. It can be seen clearly that the effect on the intensities of different peaks in XRD spectra is significantly different in distinct doping positions. In other words, the intensities in the XRD spectra vary apparently with different diffraction positions, and the variation at Li-site doping is much bigger than Fe-site. For instance, the peak intensity at 17.14° increased when doped at Fe-site, but decreased as doped at Li-site; the peak intensity at 29.70° remained unchanged when doped at Fe-site, but decreased greatly after doping Li-site; the peak intensity at 20.78° decreased only a little for doping at Fe-site, but it is very remarkable for Li-site and is the greatest of all the data in this study. As a result, the doping position and amount may be determined based on the changes of peaks.

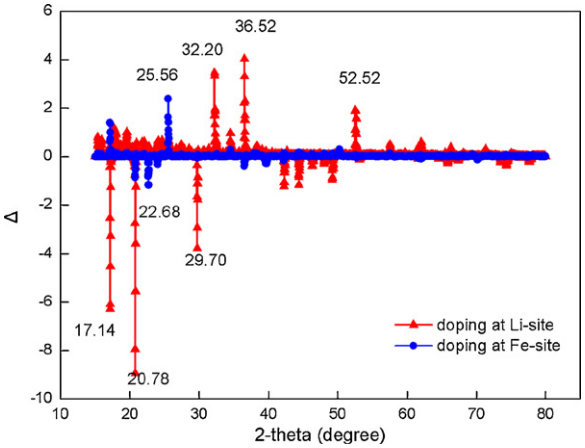

Fig. 4. The comparison chart before and after doping.

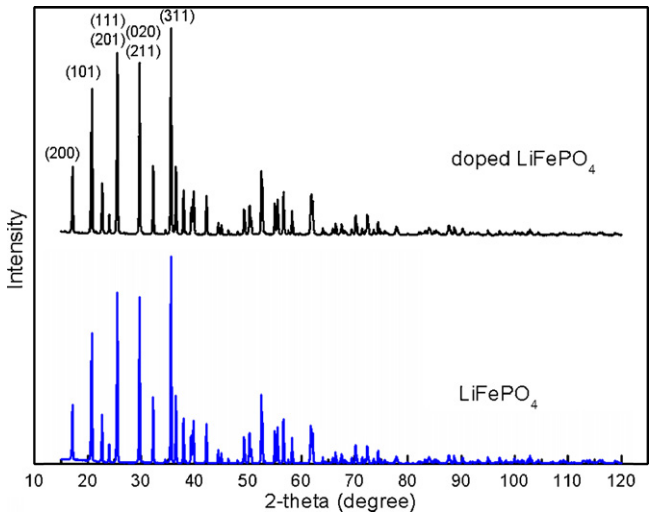

Fig. 5. XRD pattern of synthesized $LiFePO_4$.

From Fig. 4, it can be concluded that the peak intensities change significantly according to the doping positions. For Li-site doping, the peaks are 17.14°, 20.78°, 29.70°, 32.20°, 36.52°, and 52.52°, while they are 17.14°, 20.78°, and 25.56° for Fe-site doping. In other words, at 32.20°, 36.52°, and 52.52°, the intensities change more markedly for Li-site doping than Fe-site doping, whereas at 17.14°, 20.78°, 25.56°, and 29.70°, the changes for Li-site doping is relatively smaller than that in the Fe-site. By the simulation calculation, the effect of doping position on the XRD spectra can be observed.

Fig. 5 illustrates the XRD spectra of the samples synthesized in the experiment (undoped and Nb-doped $LiFePO_4$). The phase analysis was carried out based on X-ray powder diffraction patterns obtained on a Rigaku D/max 2500/PC diffractometer with Cu K radiation and graphite monochromater. The diffractometer parameters were set at 50 kV and 250 mA, scanning from 15° to 120° in 2θ with a scan step size of 0.02° and step time of 2 s. The Rietveld refinement was employed to investigate the crystal structure. The refinement terminated with $x = 0.0139(15)$, $y = 0.0681(57)$ when the Nb atoms are randomly distributed on both Fe and Li positions in $LiFePO_4$ lattice. $Li_{1-5/256}Nb_{5/256+32/256}Fe_{1-32/256}PO_4$ was used as the simulated model of doped $LiFePO_4$.

For undoped $LiFePO_4$, the diffraction peaks of experimental synthetic sample show good agreement with those of simulated sample (see Table 1), both of which also match well standard JCPDS database (PDF# 83-2092). Whereas, for Nb-doped $LiFePO_4$, there appears to be a little difference between some peaks (such as peak (2 1 0) and (2 0 0)) in the spectra of the experiment and simulated samples, which could be attributed to the resulting positive vacancy-type defects when high valent metal ions were doped into $LiFePO_4$. Since there were no peaks of impurity, and the positions of the main diffraction peaks after Nb-doping shift a little compared with the standard database, it may be concluded that Nb was inserted the internal lattice and caused a little distortion of crystal lattice, yielding the inner defects. The researches of Chung showed that the XRD pattern has no detectable impurity phases when the samples were $Li_{1-x}M_xFePO_4$.

3.2.2. Effect of different doped elements on XRD spectra

Although the amount of doping metal may be quantitatively determined by ICP measurement, however, whether the doping metal ion (or atom) is inserted into internal lattice as a replacement atom (if so, the ions/atoms occupy either Li-site or Fe-site doping, or even both), or formed the interstitial impurities, or only wrapped in the crystal surface, these issues remain to be answered. A variety

Table 1
Intensities of main peaks of simulated and experimental $LiFePO_4$.

(*h k l*)	PDF 83-2092		Experiment				Simu data			
			$LiFePO_4$		Doped-$LiFePO_4$		$LiFePO_4$		Doped-$LiFePO_4$	
	2θ	Intensity	2θ	Intensity	2θ	Intensity	2θ	Intensity	2θ	Intensity
(2 0 0)	17.15	37.94	17.14	28.70	17.14	33.48	17.16	41.80	17.16	43.58
(1 0 1)	20.77	76.18	20.76	63.08	20.76	70.93	20.78	81.66	20.78	70.90
(2 1 0)	22.68	24.22	22.68	23.69	22.70	25.21	22.70	19.31	22.68	15.87
(1 1 1)	25.56	83.28	25.56	82.56	25.58	88.24	25.58	85.14	25.58	93.86
(0 2 0)	29.71	78.18	29.70	80.63	29.72	83.56	29.72	82.50	29.72	79.34
(3 0 1)	32.21	31.23	32.22	32.17	32.22	33.66	32.24	25.86	32.22	34.98
(3 1 1)	35.58	100	35.58	100	35.60	100	35.60	100	35.60	100

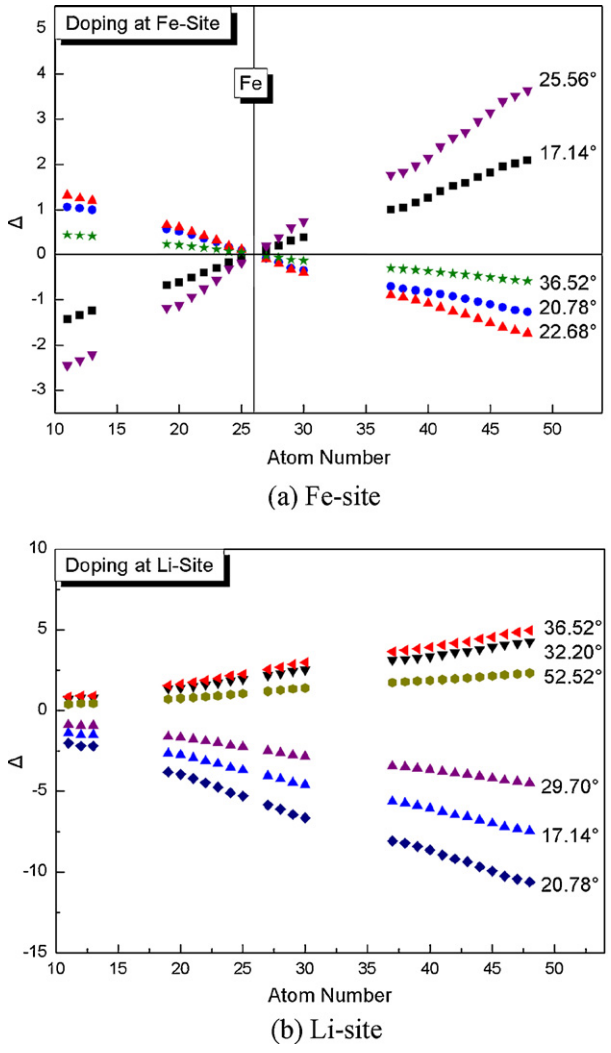

Fig. 6. The relationship between peak intensities and atomic number.

of techniques have been recently used to analyze the locations or types of different doped elements in $LiFePO_4$. For example, Wang et al. [24] investigated the Ti occupancy site in a $LiTi_{0.01}Fe_{0.99}PO_4$ sample using XANES at the Fe K-edge, it was thus suggested that Ti might replace Fe rather than Li. Xia and co-workers [32] investigated Mo-doped $LiFePO_4$ by X-ray absorption spectroscopy (XAS) experiments, and concluded that Mo ions could replace both Fe and Li ions. Wen et al. [10] studied the crystal structure of V-doped $LiFePO_4$ through the method of Rietveld refinement, and indicated that V atoms would substitute either Li or Fe atoms randomly in $LiFePO_4$ lattice.

In this paper, the XRD spectra data were obtained by simulating $LiFePO_4$ with supercell (2 2 2) in which the Li-site or Fe-site was substituted by different dopants such as alkali metals, alkaline-earth metals and transition metals in the third or fourth cycles of Periodic Table. Compared with those of undoped samples, the diffraction peaks with greatest intensity changes were investigated, and the relationship between peak intensity and atomic number was then discussed as shown in Fig. 6.

Fig. 6(a) shows the results when doped at Fe-site, we can see that the peak intensity changed almost linearly versus the atomic number of doping element (Fe is taken as the reference element), the larger the difference of atomic number between doped element and Fe, the larger the change of peak intensity, indicating the greater effect of doping on the XRD spectra. Meanwhile, the influence differs significantly with different peak positions, although the change trend is similar. For example, the intensities at 22.68° and 20.78° decrease progressively with the atomic number, while the intensities at 17.14° and 25.56° increase accordingly.

Comparatively, Fig. 6(b) gives the results when doped at Li-site, exhibiting the similar changes as Fe-site. However, as discussed previously (see Fig. 4), the influence on the intensities of main peaks is significantly different due to different doping positions. Besides, since the atomic numbers of all doping elements are larger than that of Li, the peak intensities increased linearly with the atomic numbers. Overall, the trend of intensity changes is more evident than Fe-site doping.

4. Conclusions

In this study, the XRD spectra of doped $LiFePO_4$ were simulated with the computer software. The results showed that, regardless of experimental or simulated XRD analysis, 0.02° should be selected as the suitable step size; the different positions of doping affected the XRD spectra evidently: the Li-site doping typically showed much more affection than Fe-site doping; the peak intensities varied with different doping elements, and the variation degree of intensity at different doping positions showed a linear variation with the atomic numbers of doping elements.

In summary, the computer simulation can be employed to analyze precisely doped $LiFePO_4$, and the results obtained will be expected to provide theoretical guidance for further experimental studies.

Acknowledgments

This work was financially supported by the National Natural Science Foundation of China (grant #50474092, 50874074), Natural Science Foundation of Guangdong Province (grant #8151806001000028), Shenzhen Government's Plan of Science and Technology (grant #ZYC200903250150A, 200505), and Open Research Fund of Shenzhen Key Laboratory of Functional Polymer (grant FP20090104).

References

[1] A.K. Padhi, K.S. Nanjundaswamy, J.B. Goodenough, J. Electrochem. Soc. 144 (1997) 1188–1194.
[2] B. Kang, G. Ceder, Nature 458 (2009) 190–193.
[3] X. Zhi, G. Liang, L. Wang, X. Ou, L. Gao, X. Jie, J. Alloys Compd. 503 (2010) 370–374.
[4] K. Kim, Y.-H. Cho, D. Kam, H.-S. Kim, J.-W. Lee, J. Alloys Compd. 504 (2010) 166–170.
[5] N. Ravet, Y. Chouinard, J.F. Magnan, S. Besner, M. Gauthier, M. Armand, J. Power Sources 97–98 (2001) 503–507.
[6] L. Wu, X. Li, Z. Wang, H. Guo, X. Wang, F. Wu, J. Fang, Z. Wang, L. Li, J. Alloys Compd. 506 (2010) 271–278.
[7] N. Hua, C. Wang, X. Kang, T. Wumair, Y. Han, J. Alloys Compd. 503 (2010) 204–208.
[8] D.H. Kim, J. Kim, Electrochem. Solid-State Lett. 9 (2006) A439–A442.
[9] S.B. Lee, I.C. Jang, H.H. Lim, V. Aravindan, H.S. Kim, Y.S. Lee, J. Alloys Compd. 491 (2010) 668–672.
[10] Y. Wen, L. Zeng, Z. Tong, L. Nong, W. Wei, J. Alloys Compd. 416 (2006) 206–208.
[11] X.J. Chen, G.S. Cao, X.B. Zhao, J.P. Tu, T.J. Zhu, J. Alloys Compd. 463 (2008) 385–389.
[12] J. Yao, S. Bewlay, K. Konstantionv, V.A. Drozd, R.S. Liu, X.L. Wang, H.K. Liu, G.X. Wang, J. Alloys Compd. 425 (2006) 362–366.
[13] Y.-C. Chen, J.-M. Chen, C.-H. Hsu, J.-W. Yeh, H.C. Shih, Y.-S. Chang, H.-S. Sheu, J. Power Sources 189 (2009) 790–793.
[14] A. Yamada, Y. Kudo, K.-Y. Liu, J. Electrochem. Soc. 148 (2001) A747–A754.
[15] A.Y. Shenouda, H.K. Liu, J. Alloys Compd. 477 (2009) 498–503.
[16] Y. Wang, Y. Yang, X. Hu, Y. Yang, H. Shao, J. Alloys Compd. 481 (2009) 590–594.
[17] S.-Y. Chung, J.T. Blocking, Y.-M. Chiang, Nat. Mater. 1 (2002) 123–128.
[18] D. Morgan, A. Van der Ven, G. Ceder, Electrochem. Solid-State Lett. 7 (2004) A30–A32.
[19] M.S. Islam, D.J. Driscoll, C.A.J. Fisher, P.R. Slater, Chem. Mater. 17 (2005) 5085–5092.
[20] X. Ouyang, M. Lei, S. Shi, C. Luo, D. Liu, D. Jiang, Z. Ye, M. Lei, J. Alloys Compd. 476 (2009) 462–465.
[21] C. Delmas, M. Maccario, L. Croguennec, F. Le Cras, F. Weill, Nat. Mater. 7 (2008) 665–671.
[22] M. Giorgetti, M. Berrettoni, S. Scaccia, S. Passerini, Inorg. Chem. 45 (2006) 2750–2757.
[23] A. Deb, U. Bergmann, E.J. Cairns, S.P. Cramer, J. Phys. Chem. B 108 (2004) 7046–7051.
[24] G.X. Wang, S. Bewlay, S.A. Needham, H.K. Liu, R.S. Liu, V.A. Drozd, J.-F. Lee, J.M. Chend, J. Electrochem. Soc. 153 (2006) A25–A31.
[25] G.X. Wang, S. Needhama, J. Yao, J.Z. Wang, R.S. Liu, H.K. Liu, J. Power Sources 159 (2006) 282–286.
[26] A. Nytén, J.O. Thomas, Solid State Ionics 177 (2006) 1327–1330.
[27] N. Sharma, V.K. Peterson, M.M. Elcombe, M. Avdeev, A.J. Studer, N. Blagojevic, R. Yusoff, N. Kamarulzaman, J. Power Sources 195 (2010) 8258–8266.
[28] M. Wagemaker, B.L. Ellis, D. Lützenkirchen-Hecht, F.M. Mulder, L.F. Nazar, Chem. Mater. 20 (2008) 6313–6315.
[29] J. Oddershede, T.L. Christiansen, K. Ståhl, J. Appl. Crystallogr. 41 (2008) 537–543.
[30] R. Yang, X. Song, M. Zhao, F. Wang, J. Alloys Compd. 468 (2009) 365–369.
[31] O.V. Yakubovich, M.A. Simonov, N.V. Belov, Dokl. Akad. Nauk SSSR 235 (1977) 93–95.
[32] Z.L. Wang, S.R. Sun, D.G. Xia, W.S. Chu, S. Zhang, Z.Y. Wu, J. Phys. Chem. C 112 (2008) 17450–17455.